# Gels from Modified Zirconium *N*-Butoxide: A Pyrolysis Study by Coupled Thermogravimetry, Gas Chromatographic, and Mass Spectrometric Analyses

Rosa Di Maggio,* Renzo Campostrini, and Graziano Guella†

*Dipartimento di Ingegneria dei Materiali and Dipartimento di Fisica, Università di Trento 38050 Trento, Italy*

*Received March 24, 1998. Revised Manuscript Received September 28, 1998*

A brown gel was prepared by mixing $Zr(OBu^n)_4$ and $Ce(acac)_3$ in anhydrous ethanol. The pyrolysis of this sample was followed under helium flow by online thermogravimetric (TG), gas chromatographic (GC), and mass spectrometric (MS) measurements, to study the conversion of the gel into densified powders. Two different experimental configurations (TG−MS) and (TG−GC−MS) were used for gas-phase analyses and the identification of the species evolved during thermal treatments. Mass loss occurs in five steps and the densification of the gel results from condensation reactions and from the decomposition of the acetylacetonato groups at low temperature. At higher temperature, the elimination of butene occurs from the residual butoxide left in the gel. The experimental results indicate that the gel after the analyses under helium is amorphous and crystallizes during transmission electron microscopy (TEM) observations. The temperature and atmosphere of firing have a large effect on the gel structure; this is discussed on the basis of infrared spectroscopy (IR) data.

## Introduction

$CeO_2$-stabilized tetragonal zirconia polycrystals (Ce-TZP) have been widely studied owing to their remarkable mechanical and thermal properties.[1] Despite the large interest in these materials, uncertainty still pervades the $ZrO_2$-rich zone of the $CeO_2-ZrO_2$ phase diagram. The sol−gel technique has constituted a nonconventional route to the preparation of Ce-TZP containing up to 18 mol % $CeO_2$.[2]

Protective coatings are among the most promising applications of the zirconia-based materials that are obtained from the sol−gel process.[3,4] Indeed, thin films seem to be suitable as protective layers on stainless steels and ferrous alloys against corrosion in acid environment and high-temperature oxidation. Their properties, e.g. chemical durability and high thermal shock resistance, match the requirements for a reliable protective coating. Furthermore, the similarity of thermal expansion coefficient of the Ce-TZP and stainless steel[2] reduces the thermal mismatch between coating and metallic substrate, during processing and servicing at high temperature. The protective capability of thin coatings prepared from $Zr(OBu^n)_4$ and $Ce(acac)_3$ solutions has already been tested in previous works.[4,5] Those studies have indicated that the morphologies and protective effect of the coatings strongly depend on the firing procedures, which modify the amount of the organic and hydroxylic functional groups. Coatings treated under vacuum were mostly uncracked and performed better in acidic solutions than those treated in air. The knowledge of rearrangements of organic residuals during the thermal conversion of gel into ceramic powder could elucidate the findings.

This paper reports the sol−gel characterization of a $ZrO_2-CeO_2$-based gel. Different stages from solutions of the precursors up to the thermally treated gel have been studied. The emphasis will be on the determination of the products evolved during pyrolysis of the gel, by thermogravimetric, gas chromatographic, and mass spectroscopic techniques in order to establish the mechanisms of the gel transformation.

The presence in the starting gel of the acetylacetonato ligand presumably affects the pyrolysis mechanism. To elucidate its effect, the pyrolysis of $Zr(acac)_4$ was also studied by the same procedure.

## Experimental Section

**Samples Preparation.** The chemicals used for the gel preparation were $Zr(OBu^n)_4$ (80 wt % in *n*-butanol) and $Ce(acac)_3$ anhydrous, both purchased from Sigma-Aldrich, and anydrous ethanol ($H_2O$ amount less than 0.1%) from Carlo Erba. All chemicals were used without further purification. The preparation of the solution involved first dissolving 2.87 g of $Ce(acac)_3$ into 50 mL of ethanol at room temperature. The dissolution of the compound took about 3 h under continuous stirring. Then 13.51 g of $Zr(OBu^n)_4$ was added to the solution, which was stirred until it became transparent. (In the absence of $Ce(acac)_3$, the alkoxide of zirconium readily forms an amorphous precipitate of hydrous zirconia.) The solution is stable over a long time, even years, if sealed. Otherwise, the gelation occurs in about 1 month, induced by moisture from the air (60−70% relative humidity). Subsequently the gel was

† Dipartimento di Fisica.

(1) Tsukuma, K. *Am. Ceram. Soc. Bull* **1986**, *65* (10), 1386.
(2) Scardi, P.; Di Maggio, R.; Lutterotti, L.; Maistrelli, P. *J. Am. Ceram. Soc.* **1992**, *75*, 2828.
(3) De Lima Neto, P.; Atik, M.; L. Avaca; Aegerter, M. A. *J. Sol-Gel Sci. Technol.* **1994**, *1*, 177.
(4) Di Maggio, R.; Fedrizzi, L.; Rossi, S.; Scardi, P. *Thin Solid Films* **1996**, *286*, 127.
(5) Di Maggio, R.; Fedrizzi, L.; Rossi, S.; Scardi, P. *Surf. Coat. Technology* **1997**, *89*, 292.

10.1021/cm980187h CCC: $15.00 
Published on Web 11/21/1998

dried at 80 °C for 2 h and used for the pyrolysis characterization. The calcination, which involved placing the gel directly into a hot furnace at 400 °C for 30 min in air, furnished a yellow powder.

Furthermore two samples were also prepared by different heat treatments of the gel. The first sample was obtained by placing the gel in a cold furnace up to 400 °C in air; the second one was prepared by heating the gel up to 500 °C in a vacuum. In both of the last cases the heating rate was 20 °C/min.

**Instrumentation.** Surface area measurements were performed with a Sorptomatic 1800 Carlo Erba instrument, based on the adsorption isotherms of nitrogen at 77 K. A static-volumetric technique was used, which measures the adsorbed gas volumes from pressure changes, according to the Brunauer–Emmett–Teller (BET) method.

Infrared (IR) spectra were recorded in the transmission mode (on KBr pellets) using a FT-IR Nicolet spectrophotometer. Thermal analyses were performed on a Netzsch STA 409 simultaneous analyzer. Thermogravimetry (TG), derivative thermogravimetry (DTG), and differential thermal analysis (DTA) were recorded in the range 20–1000 °C both in air and under helium flow (100 mL $min^{-1}$) at a heating rate of 10 °C $min^{-1}$. Powder samples were placed in alumina crucibles, using $\alpha$-$Al_2O_3$ as a reference. Analyses were performed on an HRGC gas chromatograph (Carlo Erba Instruments) with a VG QMD1000 quadrupole mass spectrometer as detector. Chromatographic analyses were carried out by using He as carrier gas with a inlet pressure of 40 kPa. Volatile oxygen-containing compounds and light hydrocarbons were eluted and well resolved in a PoraPLOT Q capillary column (25 m × 0.32 mm) (Chromopack). The chemical species detected by chromatographic analyses were labeled on the basis of their relative retention times as referred to the air peak.

Electron impact mass spectra (70 eV) were continuously recorded and stored, with scans from 3 to 400 amu. Each scan was recorded in 0.9 s with a delay time of 0.1 s. Gas chromatographic analysis was recorded using the total ion current (TIC) of each scan. The coupled configuration (TG–MS) allowed us (a) to analyze mass spectra recorded vs time, i.e., vs pyrolysis temperature, (b) to reveal the presence of the evolved gaseous species from the shape of the TIC curve, obtained from the contribution of each recorded scan, and (c) to follow the ion current of a single proper *m*/*z* value which may represent the evolution, as a function of the temperature, of a particular molecular species. The use of TG–MS was already introduced for studying the thermolysis of polysiloxane resins.[6,7] The configuration (TG–GC–MS) allows us also to better identify the pyrolysis products simultaneously evolved during the main weight losses of the gel.[8] With this kind of instrumental configuration, chemical species were first separated by chromatographic elution and then identified on the basis of both their mass spectra and relative retention time.

For transmission electron microscopy (TEM) observations a Phillips 400T microscope operated at 120 keV were used. Powder specimens were suspended in ethanol and spread onto a copper grid covered with an amorphous carbon film.

## Results and Discussion

**Chemical Modification of Precursors and Gel Characterization.** The solution containing $Zr(OBu^n)_4$ and $Ce(acac)_3$ is transparent and does not form hydrous zirconia precipitates up to gelation and thus behaves differently from the solution containing only the zirconium alkoxide. Hence a ligand exchange must be supposed: the alkoxide of zirconium expands its coordination sphere via acac chelating ligands.[9,10] The modification of zirconium was indicated by the solution color turning from pale yellow to orange-brown. By ligand exchange the reactivity toward hydrolysis, solvolysis, and condensation of both the zirconium and cerium species is modified.

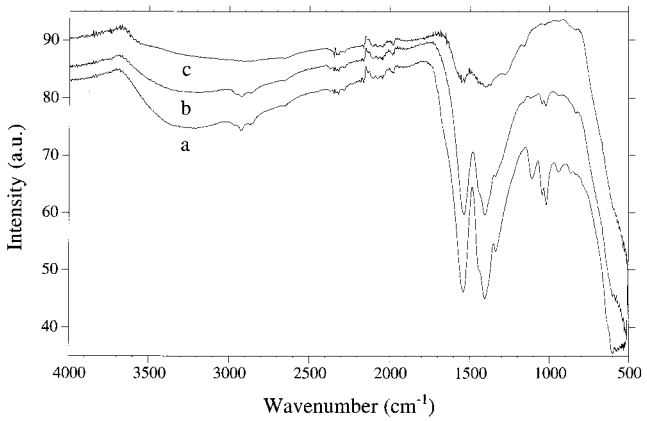


**Figure 1.** IR spectra of the gel pyrolized at 260 (a), 350 (b), and 450 (c) °C.

**Scheme 1**

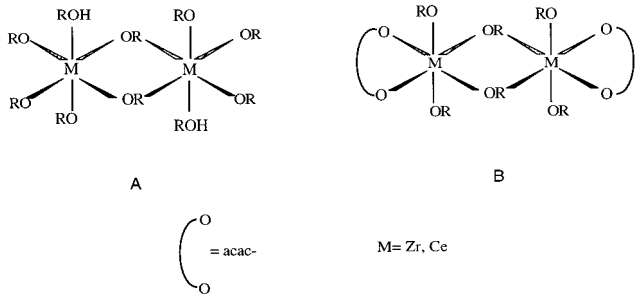


In this regard, changes in the local structure of cerium(IV) and zirconium(IV) have been characterized by means of EXAFS spectroscopy and supported by FT-IR analyses.[11–16] The dimeric species (A), indicated in Scheme 1, is claimed to be in fast equilibrium with the trimeric form for $M(OR)_4$ in its parent alcohol when M = Zr(IV) but with the monomer when M = Ce(IV). Moreover, the acetylacetone (acacH) reacts with the alkoxides, forming species (B) (Scheme 1), whose amount depends on the modification ratio $r$ = [acac]/[M]. In absence of any modification or for $r = 0.1$, the dimeric species (A) is the main precursor, showing a high rate of hydrolysis and condensation. Under these conditions only a precipitate of hydrous oxide should be formed. For $r$ values up to 1, the amount of species B increases and determines the hydrolysis and condensation rate, yielding first colloidal suspensions and then, after aging,

(6) Belot, V.; Corriu, R. J. P.; Leclercq, D.; Mutin, P. H.; Vioux, A. *J. Mater. Sci. Lett* **1990**, *9*, 1052.
(7) Bouillon, E.; Langlais, F.; Pailler, R.; Naslan, R.; Cruege, F.; Sarthou, J. C.; Delpuech, A.; Laffon, C.; Lagarde, P.; Monthioux, M.; Oberlin, A. *J. Mater. Sci.* **1991**, *26*, 1333.
(8) Campostrini, R.; D'Andrea, G.; Carturan, G.; Ceccato, R.; Sorarù, G. D. *J. Mater. Chem*. **1996**, *6* (4), 585.
(9) Chatry, M.; Henry, M.; In, M.; Sanchez, C.; Livage, J. *J. Sol-Gel Sci. Tech*. **1994**, *1*, 233.
(10) Debsikdar, J. C. *J. Non-Cryst. Solids* **1986**, *87*, 343.
(11) Papet, P.; Lebars, N.; Baumard, J. F.; Lecomte, A.; Dauger, A. *J. Mater. Sci.* **1989**, *24*, 3850.
(12) Ribot, F.; Toledano, P.; Sanchez, C. *Chem. Mater*. **1991**, *3*, 759.
(13) Peter, D.; Ertel, T. S.; Bertagnolli, H. *J. Sol-Gel Sci. Technol.* **1994**, *3*, 91.
(14) Peter, D.; Ertel, T. S.; Bertagnolli, H. *J. Sol-Gel Sci. Tech*. **1995**, *5*, 5.
(15) Léaustic, A.; Babonneau, F.; Livage, J. *Chem. Mater.* **1989**, *1*, 240.
(16) Léaustic, A.; Babonneau, F.; Livage, J. *Chem. Mater.* **1989**, *1*, 248.

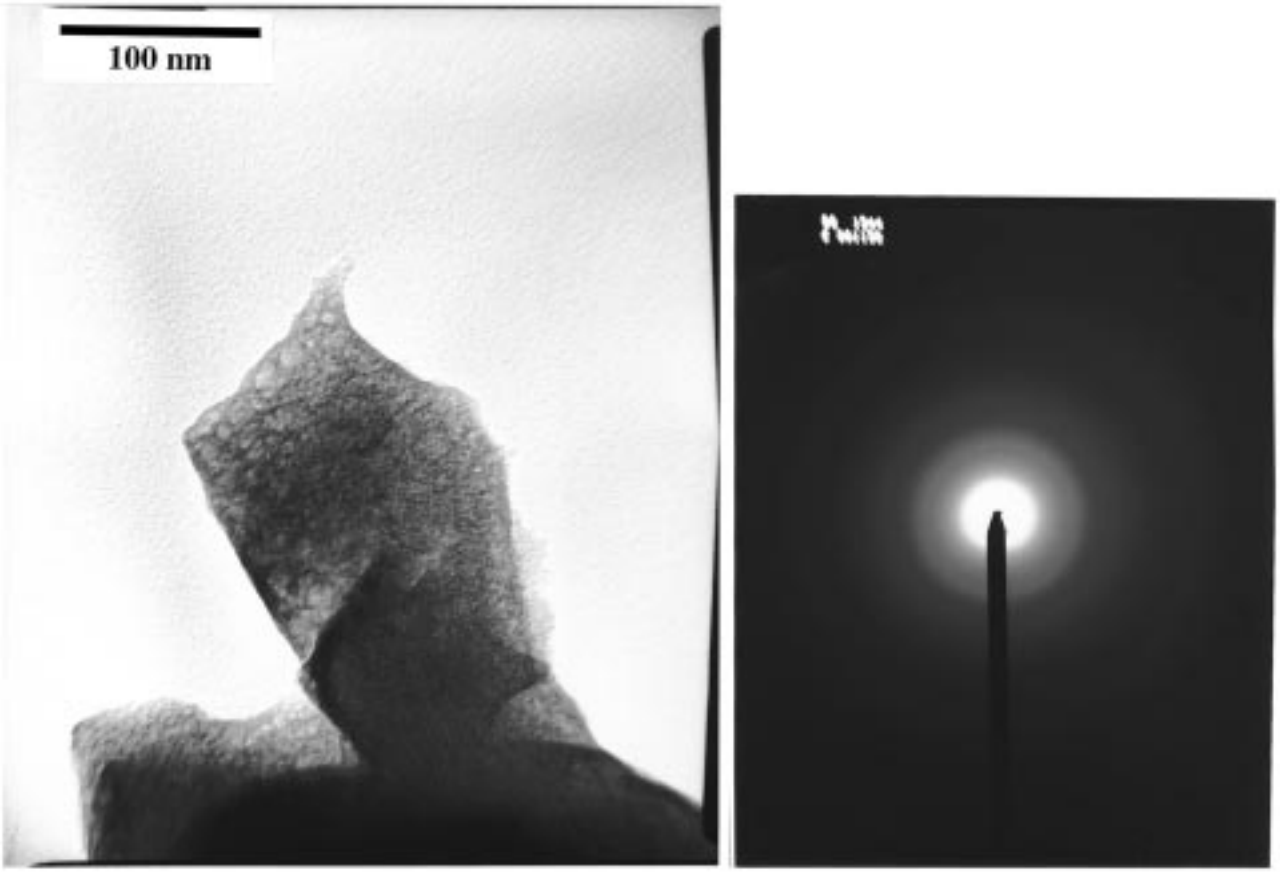


**Figure 2.** TEM micrograph and SAD pattern showing the amorphous structure of the gel.

transparent gels. In this range of ligand concentration, the gel varies between branched polymers to a highly open structure. Upon hydrolysis, most of the alkoxy groups are removed, while the chelating ligands remain. For r > 1, condensation becomes the slow process, as the bulky complexing ligands, still bonded to zirconium or cerium and located on the surface of weakly condensed species, avoid further condensation. This results in the formation of molecular compounds, which cannot undergo gelation even after long times.[11,12]

After the ligand exchange between $Ce(acac)_3$ and $Zr(OBu^n)_4$, in the starting solution the modification ratio $r = [acac]/[Zr + Ce]$ corresponds to a value of 0.55. This solution forms a brown, transparent gel in a few weeks of aging at room temperature, in good agreement with the previous model. In fact the decrease of the functionality of the acetylacetonato-modified precusors, because of the low reactivity of the acac ligand toward hydrolysis, leads to the formation of highly branched macromolecules.

Although the hydrolysis was performed by moisture from the air, most of the alkoxy groups are removed. In fact, the chemical analysis of the dried gel gives for C, H, Ce, and Zr a wt % of 16.76, 2.03, 13.53, and 42.63, respectively. These results lead to a chemical composition close to $ZrCe_{0.21}O_{2.01}(acac)_{0.6}(OH)_{0.01}(H_2O)_{0.09}$, indicating that all the acetylacetonato ligands remain chelated to metal atoms after hydrolysis and condensation. Actually a second composition, $ZrCe_{0.21}O_2(acac)_{0.5}(OBu^n)_{0.11}(OH)_{0.02}(H_2O)_{0.16}$, is consistent with the results of the chemical and thermal analyses, suggesting that if most of the acac is preserved in the solid, also a few butoxy groups still remain in it. Consequently, to establish the nature of organic residuals, the IR spectra of the as prepared gel and the gel after heat treatments at increasing temperatures were collected. In Figure 1a is shown the IR spectrum of the gel after a treatment in $H_2$ at 260 °C, similar to the spectrum of the untreated gel. The broad band centered at 3374 $cm^{-1}$ for the OH stretching and the peaks corresponding to the C−H bond stretchings at 2953, 2926, and 2957 $cm^{-1}$ can be clearly detected. The strong broad peak at 1550 $cm^{-1}$ is assigned to a group of peaks related to the stretching of the C−O + C−C bonds of acetylacetonato ligands coordinated to the different metals. The three strong overlapping peaks between 1460 and 1340 $cm^{-1}$ can be ascribed to the bending of the C−H bond in $CH_3$ groups present in all species. Minor peaks can be seen at lower wavenumber values (1047−1026 and 613 $cm^{-1}$) and associated with the stretching of C−O and M−O bonds, respectively, of $OBu^n$ groups. This observation confirms that some butoxy groups are mantained in the solid. Moreover, the same peaks are also present in the spectrum of the sample treated in He at 350 °C (Figure 1b), even though the details are less pronounced. The third spectrum of Figure 1 just indicates the presence of organic species after the heat treatment in He at 450 °C.

The as prepared gel is brittle with a surface area value of 95 $m^2\ g^{-1}$, and its specific pore volume was equal to 0.6 $cm^3\ g^{-1}$. The total porosity is around 2% and the pores have radii below 6 nm, in agreement with the values measured during TEM observations. The latter also confirmed that the gel is amorphous: the

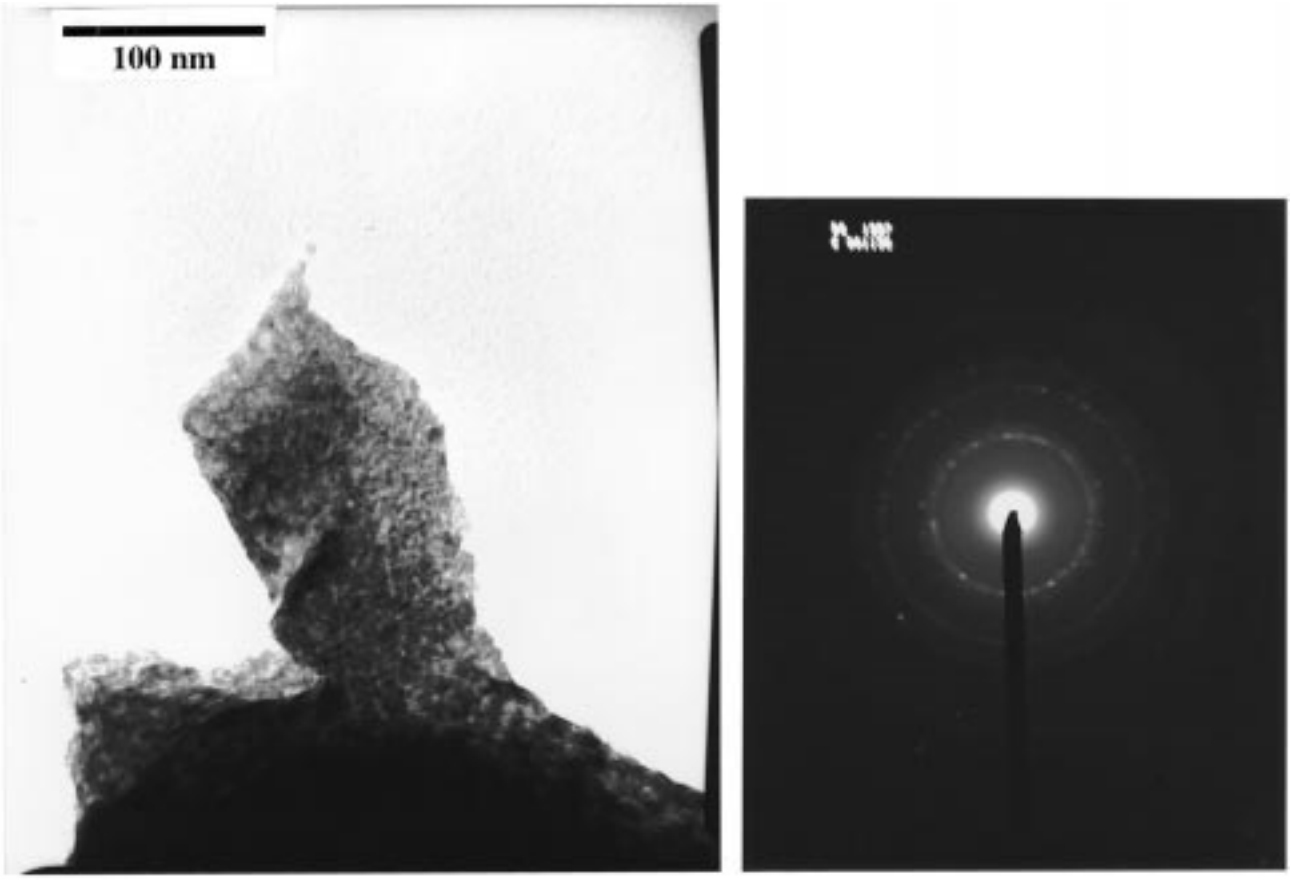


**Figure 3.** TEM micrograph and SAD pattern of the gel after prolonged electron irradiation inside the microscope.

**Table 1. Thermogravimetric Data of Pyrolysis of Gel and Corresponding Chemical Species Detected by TG−GC−MS Analyses**

| mass loss step | mass loss intensity (%) | sampling temp (°C) | species detected |
|---|---|---|---|
| I | 4.3 | 120 | $H_2O$ |
| II | 3.6 | 260 | $CO_2$, $H_2O$ (minor $CH_3COOH$, $(CH_3)_2CO$, $CH_3COC_2H_5$) |
| III | 9.5 | 350 | CO, $CO_2$, $H_2O$ (minor $(CH_3)_2CO$, $CH_3COC_2H_5$, $CH_3COC_3H_7$,$CH_3COOH$) |
| IV | 4.2 | 450 | $CO_2$, $H_2O$ (minor $CH_3COOH$, $(CH_3)_2CO$, $CH_3COC_2H_5$, $CH_3COC_3H_7$, butene, aromatics) |
| V | 1.3 | 560 | $CO_2$ (minor $H_2O$, $(CH_3)_2CO$, $CH_4$, $CH_3CH_3$, $CH_3COOH$, $CH_3COC_2H_5$) |

micrograph and relevant pattern is shown in Figure 2. Actually, faint diffraction rings can be seen in the pattern, probably determined by a very early stage of crystallization induced by in situ electron beam irradiation. In fact, the microstructure of the powder was not stable under prolonged electron irradiation, as shown in Figure 3, so the mild heating in air yields the crystallization of the gel, meanwhile $Ce^{3+}$ ions oxidize into $Ce^{4+}$. The so-obtained crystalline phase can be identified as tetragonal $ZrO_2-CeO_2$, with domains in the 5−12 nm range, which do not enlarge further under subsequent electron irradiation.

TG−DTG analyses of the gel carried out in air (not presented) showed a mass loss occurring in three subsequent steps of 2.6, 21.6, and 0.6%, centered at 120, 250, and 500 °C, respectively. Corresponding to the large mass loss, the DTA curve showed a strong, narrow, and exothermic peak, due to the combustion of organic residuals.

As evidenced by the TEM observations, also the yellow crystalline powder, obtained from the calcination of the gel, consists of finely distributed $ZrO_2-CeO_2$ crystallites, having dimensions ranging from 2 to 7 nm. The diffraction patterns of the crystalline sample can be indexed according to the $ZrO_2-CeO_2$ tetragonal phase, even though they would be also compatible with the cubic one, as reported in the literature for similar systems.[17] The uncertainty arises both from the similarity of the diffraction pattern for the two phases or the possible coexistence of the cubic and tetragonal crystallites in the examined samples. In fact, the tetragonal phase can easily form from the cubic one by simple strains as induced by the release of organics or $H_2O$ during condensation reactions.

**Gel Pyrolysis.** A better understanding of the gel structure and the nature of the organic residuals was achieved from its pyrolysis in He up to 1000 °C. The TG analysis shows a continuous mass loss from 40 to 740 °C. The curve was characterized by several slope values, suggesting that different processes contributed to the whole loss. Five different steps of 4.3, 3.6, 9.5, 4.2, and 1.3% mass loss at 120, 260, 360, 450, and 620 °C, respectively, could be detected by DTG. DTA analysis showed two endothermal broad peaks at 130 and 320 °C.

Continuous mass spectral analyses of the gases evolving during pyrolysis provided a TIC curve (Figure 4)

(17) Nagarajan, M. S.; Rao, K. J. *J. Mater. Sci.* **1989**, *24*, 2140.

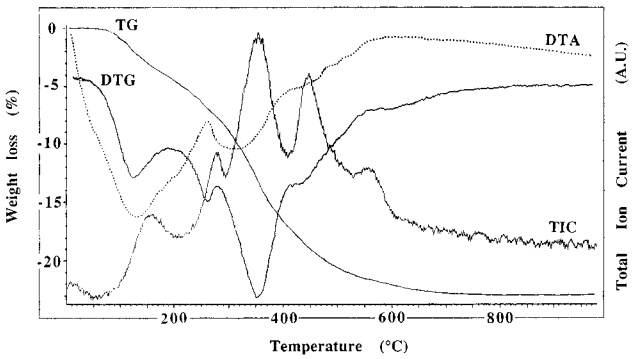


**Figure 4.** TIC, DTA, TG, and DTG curves of sample gel in He (see the text).

showing five fairly resolved bands, whose maxima were at the same temperatures as the DTG signals and selected for gas-chromatographic sampling in TG−GC−MS analyses. The related chromatograms are shown in Figure 5, whereas Table 1 summarizes the intensity and temperatures of the mass losses and the chemical species evolved during the pyrolysis.

The first weight loss at 120 °C is mainly assignable to the release of $H_2O$, probably trapped inside the porous gel network, although the sample was dried at 80 °C for a few hours before the analyses. A further contribution to the release of $H_2O$ comes from the condensation of two M−OH moieties with the formation of oxo bridges. This reaction causes a second minor water evolution at 260 °C, as evidenced from the trend of 18 *m*/*z* ion vs temperature (Figure 6). In fact the contribution to the ion current of the 18 *m*/*z* value, which corresponds to the parent ion of $H_2O$, shows a peak at 130 °C with a shoulder at 260 °C, relating to the first and second peaks in the TIC curve, respectively. The absence of EtOH in the evolved gases shows that either the solvent had a weak solvolysis ability or the ethoxides were hydrolyzed in solution more easily than any other ligand.

The network of the gel could be depicted as a branched inorganic polymer, where the acac ligands are the terminal groups of the chains.[18] Due to the low complexation ratio ($r = 0.55$), the inorganic metal−oxo polymer might have a large spatial extension and contain, as indicated by the IR data, some isolated butoxide groups still bonded to zirconium and cerium. Anyway, the evolution of the parent alcohols, expected to some extent on the basis of previous studies on gels derived from alkoxides of Si and Ti,[8,19] is surprisingly not observed at any temperature. Presumably due to the steric hindrance of the butyl chains and the absence of close OH groups, the butoxide groups cannot yield the alcoxolation (eq 1). Their consumption might take

$$\equiv\text{Zr-OH (s)} + \text{CH}_3(\text{CH}_2)_2\text{CH}_2\text{-O-Zr}\equiv\text{ (s)} \xrightarrow{-X-} \equiv\text{Zr-O-Zr}\equiv\text{ (s)} + \text{CH}_3(\text{CH}_2)_2\text{CH}_2\text{-OH (g)} \quad (1)$$

place through a different route at higher temperature, when the decomposition of the acetylacetonato ligands reduces the steric hindrance around the metal atom. (From now on, the reactions are proposed for zirconium due to their abundance and extended to cerium with a few precautions.)

To evaluate the trend of the acetylacetonato pyrolysis, the evolution of $(CH_3)_2O$ and $CH_3COOH$ has to be followed, since these are the main products attributable to the thermal decomposition of the chelating groups. In this regard, the presence of water seems to yield first acetic acid from acac ligands bonded to zirconium, according to the reaction 2. In fact, as can be noticed from Figure 6, the acetic acid evolution reaches its maximum already at 300 °C, which is followed by evolution of the acetone, which is given off immediately after, as proposed in reaction 3. Both of the compounds feature the second weight loss.

$$\equiv\text{Zr-OC(CH}_3\text{)CHCOCH}_3\text{ (s)} + \text{H}_2\text{O (g)} \longrightarrow \equiv\text{Zr-OC(CH}_3\text{)CH}_2\text{ (s)} + \text{CH}_3\text{COOH (g)} \quad (2)$$

$$\equiv\text{Zr-OC(CH}_3\text{)CH}_2\text{ (s)} + \text{H}_2\text{O (g)} \longrightarrow \equiv\text{Zr-OH (s)} + \text{CH}_3\text{COCH}_3\text{ (g)} \quad (3)$$

The observed higher amounts of $(CH_3)_2CO$ and $CO_2$, with respect to the other species, suggest that they arise also from a concerted reaction involving two close acac groups, according to the following simplified eq 4.

$$2\equiv\text{Zr-OC(CH}_3\text{)CHCOCH}_3\text{ (s)} + 2\text{ H}_2\text{O (g)} \longrightarrow \equiv\text{Zr-O-Zr}\equiv\text{ (s)} + 3\text{ (CH}_3\text{)}_2\text{CO (g)} + \text{CO}_2\text{ (g)} \quad (4)$$

However, these processes cannot describe the overall acac pyrolysis, and other minor reactions must be considered in order to explain the presence of the other minor chemical species detected in the TG−GC−MS analyses. For instance, the 2-butanone occurrence could be due to the 1−2 methyl migration along the carbon chain of acetylacetonato ligand and the elimination of CO (process 5).[19]

$$\equiv\text{Zr-O-C(CH}_3\text{)CHCOCH}_3\text{ (s)} + \text{H}_2\text{O (g)} \longrightarrow \equiv\text{Zr-OH (s)} + \text{CO(CH}_3\text{)CH}_2\text{CH}_3\text{ (g)} + \text{CO (g)} \quad (5)$$

At 350 °C the gas chromatogram (Figure 5) presents a large number of signals. All the reactions, invoked to explain the second mass loss, occur at 350 °C to a greater extent, so that the third weight loss is also the most conspicuous. CO, $CO_2$, and $H_2O$ were the most significant species evolved along with $(CH_3)_2CO$, $CH_3COC_2H_5$ and traces of $CH_3COOH$ and $CH_3COC_3H_7$. As the atmosphere becomes increasingly reducing, because of the pyrolysis of bulky organic residuals under an inert atmosphere, a larger variety of products are given off by the pyrolysis. In this regard, a slightly reducing environment could account for the reduction of one of the two carbonyl groups of the acetylacetonato ligands, yielding the observed traces of 2-pentanone ($t_r = 48$). The trend of this last species (*m*/*z* 86) is similar to that

(18) Sanchez, C.; In, M. *J. Non-Cryst. Solids* **1992**, *147&148*, 1.
(19) Marci, G.; Palmisano, L.; Sclafani, A.; Venezia, A. M.; Campostrini, R.; Carturan, G.; Martin, C.; Rives, V.; Solana, G. *J. Chem. Soc. Faraday Trans.* **1996**, *92 (5)*, 819.

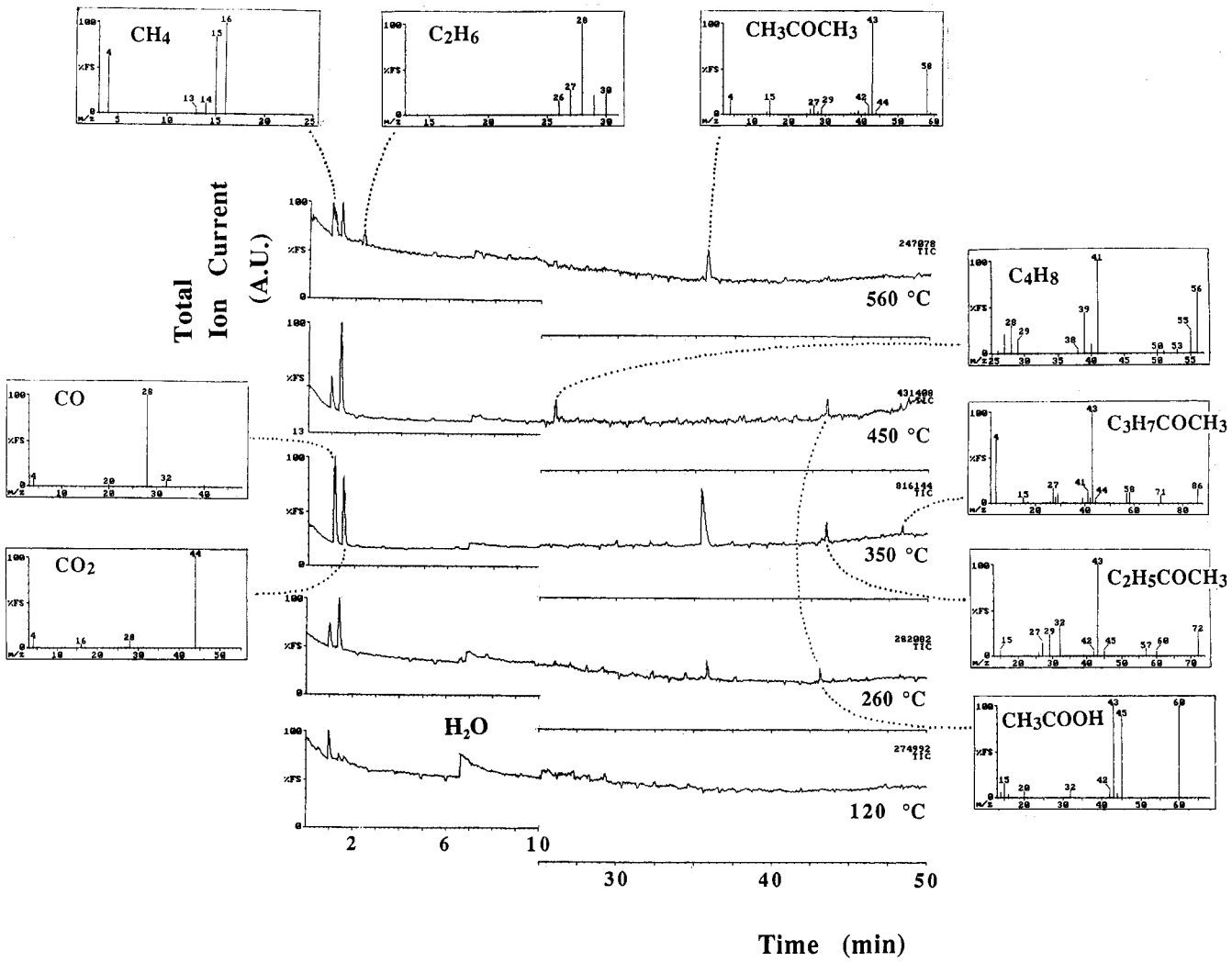


**Figure 5.** Gas chromatograms at the sampling temperatures of species eluted from the pyrolysis of gel.

of 2-butanone and acetone, indicating that acac must be the parent species.

The fourth weight loss at 450 °C shows some differences. An extension of decomposition of the acetylacetonato residuals is ascertained by the detection of the $(CH_3)_2CO$, $CH_3COC_2H_5$, $CH_3COOH$, and in traces of $CH_3COC_3H_7$.

Besides this, the main observed phenomenon regards the elimination of butene (eq 6), arising from butoxide residuals as previously discussed.

$$\equiv Zr\text{-}O\text{-}(CH_2)_3\text{-}CH_3 \longrightarrow Zr\text{-}OH + CH_2{=}CH\text{-}CH_2\text{-}CH_3 \quad (6)$$

Actually, at this temperature traces of aromatic hydrocarbons also may be detected. The trends of molecular ion peaks vs temperature of aromatic species such as benzene (*m*/*z* 78), toluene, xylene, and trimethylbenzene are similar. These products are presumably obtained from multistep processes, mainly thermal cycloaddition. This occurs from concerted reaction of two or more acac groups with formation of more stable and less oxidized intermediates, which decompose also forming aromatic compounds. For instance, the solid compound $\equiv ZrOC(CH_3)CH_2$, formed after process 2, likely reacts at higher temperature according to eq 7, rather than to give off acetone.

$$3 \equiv Zr\text{-}OC(CH_3)CH_2\,(s) \longrightarrow 3 \equiv Zr\text{-}OH\,(s) + C_9H_{12}\,(g) \quad (7)$$

Similar processes can be claimed in order to describe the formation of benzene, toluene, and xylene.

At 560 °C, $(CH_3)_2CO$ and simple hydrocarbons, i.e. $CH_4$ and $CH_3CH_3$, are the main species in the gas phase. Concerning this, the dismutation of acetylacetonato ligand could account for the evolution at high temperature of $CH_4$, as described by process 8.

$$\equiv Zr\text{-}O\text{-}C(CH_3)CHCOCH_3\,(s) + H_2O\,(g) \longrightarrow \equiv Zr\text{-}OH\,(s) + (CH_3)_2CO\,(g) + CO_2\,(g) + CH_4\,(g) \quad (8)$$

Meanwhile, the reducing environment might promote its reduction and decomposition to ethane and acetone, as described by process 9.

$$\equiv Zr\text{-}O\text{-}C(CH_3)CHCH_2CH_3\,(s) + H_2O\,(g) \longrightarrow \equiv Zr\text{-}OH\,(s) + (CH_3)_2CO\,(g) + C_2H_6\,(g) + H_2\,(g) \quad (9)$$

These reactions involve some acac groups that are maintained by the solid and subsequently decompose at high temperature. The existence of acetylacetonato

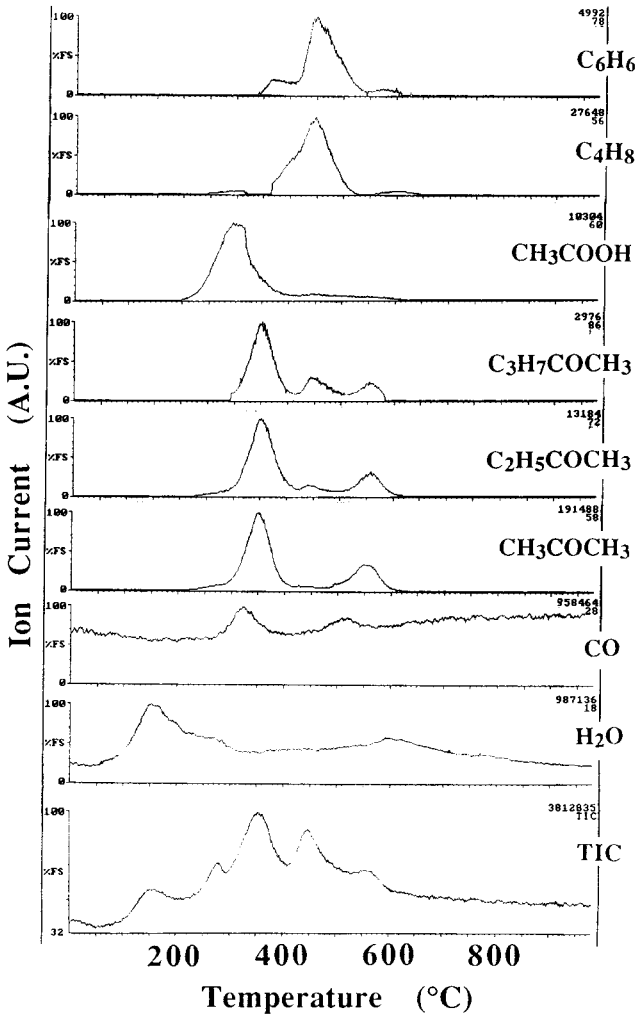


**Figure 6.** Gel *m*/*z* curves.

ligands also at high temperature could be confirmed by the evolution of $CH_3COOH$ and $CH_3COC_2H_5$, even if in traces. Moreover, the profile of the *m*/*z* 58 peak, related to $(CH_3)_2CO$ evolution (Figure 6), shows two maxima at 350 and 560 °C, suggesting a bimodal decomposition of acetylacetonato ligands due to different mechanisms that are active with the increase of the temperature.

With the aim of elucidating the mechanisms of acetylacetonato decomposition, the pyrolysis of pure Zr(acac)$_4$ was followed by TG−MS. In Figure 7 the recorded TIC curve and some representative mass spectra are shown, indicating that acacH was the single product of decomposition at low temperature (210 °C). The absence of $H_2O$ signals in the mass spectra for that temperature suggests that the acacH cannot come from the hydrolysis of acac groups. The modification of the compound is clearly observed in the IR spectrum at this temperature, where the typical strong vibrations bands, at 1520−1580 $cm^{-1}$, of the enolic form of acac have disappeared, merging into a single peak at 1586 $cm^{-1}$. A further evolution of acacH was observed at about 270 °C, accompained by acetone. The IR spectrum of the sample treated at this temperature is similar to the previous one, but shows a weak peak at 1650 $cm^{-1}$, possibly related to the presence of a C=C bond. Hence the role of zirconium should be invoked in the formation of stable unsaturated intermediates, which decompose at higher temperature, leading to aromatic species.[20] In fact, at 440 °C the mass spectra clearly show $CO_2$, acetone, and trimethylbenzene. The formation of aromatic compounds (benzene and mainly toluene, xylene, and trimethylbenzene) was more enhanced at 540 °C. Moreover, the evolution of $CH_4$, $C_2H_6$, CO, and $H_2O$ was also observed at this temperature. The formation of methane, ethane, and aromatics must be ascribed to acac groups, given they are the only species present in the solid, while no butene evolution was detected. These results provide a good confirmation that the stoichiometry of the gel and the pyrolysis processes are close to the proposed ones.

**Gel-Derived Samples.** On the basis of the previous results it can be also deduced that the structure of the gel and its organic load can be modified by adjusting the temperature and atmosphere of the thermal treatments.

As an example, when the calcination of the gel is performed by heating from room temperature up to 400 °C, the organic residuals cannot ignite but only partially burn out, yielding a brown powder. In fact, the outer material provides a barrier against oxygen diffusion toward the interior, which effectively undergoes a thermal decomposition in a nonoxidizing environment. The surface area of the sample so obtained is 80 $m^2\ g^{-1}$. It contains very small pores, having an average radius of 6 nm, along with macropores with an average radius of 1000 nm. The IR analysis of the sample (Figure 8 a) indicates that a large decrease in the amount of acac ligands occurred during the thermal treatment, presumably according to processes 2−4. Meanwhile the presence of peaks at 1020−1060 $cm^{-1}$, attributable to the butoxide groups, indicate that these organics are still present in the network, because the heat treatment did not reach the temperature at which they could be released as butene. The TG−DTG in air of the sample displayed a large mass loss from room temperature to 800 °C, consisting of two significant weight losses of 4.6 and 7.9% centered at 120 and 350 °C, respectively. The temperature of the second peak, attributable to the combustion of the organics, is higher than that recorded for the as-prepared gel (250 °C). This suggests that the organic moieties have rearranged into more reduced and stable ones during the thermal treatment up to 400 °C. Also in the TG−DTG curves recorded during the pyrolysis in a He atmosphere, two weight losses were detected: 3.6% (20−300 °C) and 4.4% in the range 300−600 °C. TG−MS analysis of gases evolved resulted in a TIC curve showing only two bands, centered at 130 and 470 °C. The MS spectra recorded at 130 °C shows $H_2O$ and $CO_2$, whereas the scan at 470 °C displayed several species, including CO, $CO_2$, $CH_4$, and traces of alkenes and aromatics. It turns out that $(CH_3)_2CO$ and $CH_3COOH$ are absent, confirming that most of the acac groups has been consumed, where the remaining have undergone a more drastic decomposition.

On the other hand, the gel treated under vacuum up to 500 °C showed a lower amount of porosity, including very small pores, with radii in the 1−6 nm range, and others having an average radius larger than 100 nm. The measured surface area is 10 $m^2\ g^{-1}$. The TG−DTG

(20) Di Maggio, R.; Fambri, L.; Guerriero, A. *Chem. Mater.* **1998**, *10*, 1777.

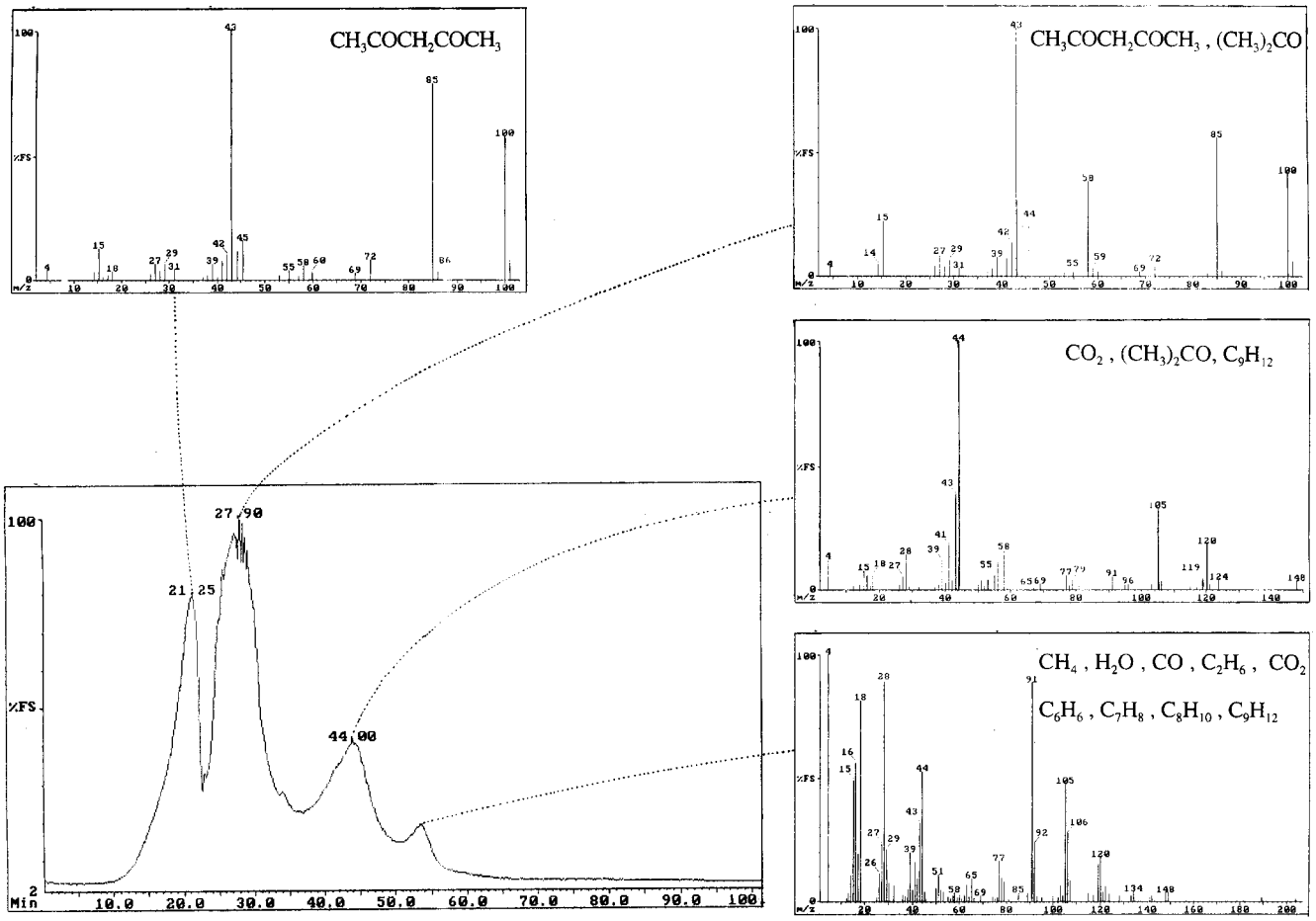


**Figure 7.** TIC (percentage vs time; temperature = time × 10) and mass spectra of the species eluted at the different temperatures during the pyrolysis of $Zr(acac)_4$.

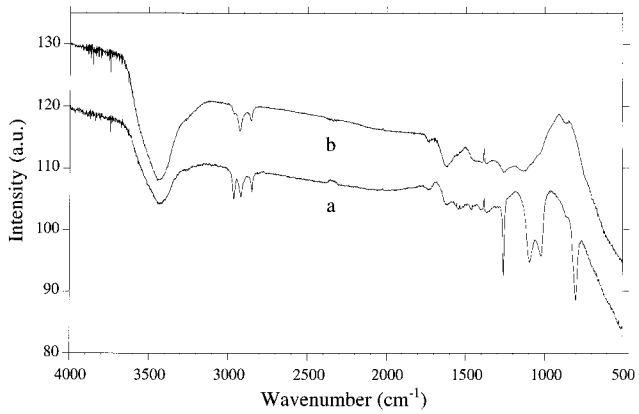


**Figure 8.** IR spectra of the gel treated at 400 °C for 30 min (a) and in a vacuum at 500 °C (b).

in air shows a decrease of weight in three steps of 0.6% (25−250 °C), 10.1% (250−420 °C), and 0.4% (420−600 °C), the second of which is due to the combustion of the organic groups and corresponds to the narrow exothermic peak at 370 °C in the DTA curve. The TG−DTG analysis performed in He showed two mass losses: the first of which (1.8%) is in the range from 25 to 280 °C and the second of 2.7%, from 280 to 760 °C. The evolution of a simple hydrocarbon, namely $CH_4$, in the gas phase is the main feature of the pyrolysis. Hence, the structure of the gel network seems to be remarkably changed during the treatment under vacuum at 500 °C. During this treatment, the residual organics underwent

**Table 2. Mass Loss (%) of Gel Samples in Air and in He**

| sample | He | air |
|---|---|---|
| gel as prepared | 22.6 | 25.0 |
| gel treated at 400 °C (static air) | 7.4 | 12.5 |
| gel treated at 500 °C (vacuum) | 4.5 | 11.1 |

reforming reactions, releasing $H_2$, and reduction, while the carbon has segregated into unsaturated structures.

The TEM observations indicate also that the two samples are initially amorphous but highly unstable under irradiation, where an early crystallization can be evidenced. In Table 2 the mass losses during pyrolysis for the as-prepared gel and the two gel-derived samples are presented. As the mass loss in air recorded for the gel is supposed to be equal to the whole initial organic content, it can be concluded that the chosen thermal treatments for the gel appear to be effective in preserving the organic moieties, in accordance with the IR patterns (Figure 8a,b). These also indicate that some hydroxyl functionalities are present too. The presence of organic in the gel-derived samples can be associated with open structures, which can lead to lower stiffness and hardness of the amorphous network with respect to the perfectly crystallized sample. The results of previous studies on $SiO_2$ gel coated glass[21,22] proved that the different properties among xerogels with different

(21) Dal Maschio, R.; Pegoretti, A.; Rizzo, C.; Sorarù, G. D.; Carturan, G. *J. Am. Ceram. Soc.* **1989**, *72*, 2388.

(22) Di Maggio, R.; Campostrini, R.; Carturan, G. *J. Mater. Sci. Lett.* **1995**, *14*, 1591.

skeletal density resulted in different resistance against crack formation, which increases when the hardness and stiffness of the coatings decrease. As a general feature, all the properties of the xerogel depend on its degree of condensation. On the other hand, especially in the case of coatings, the hydrolysis and condensation, promoted by the environment and the acid catalysis with the formation of M−O-M bonds, led to more interconnected strucures.

## Conclusions

The study of the pyrolysis process by coupling TG−GC−MS measurements, along with more conventional analyses, allowed us to obtain information about the gel structures and the nature of the organic residuals and some insight into the reactions occurring during the thermal treatments.

The formation of a gel instead of a precipitate in the starting solution is due to the ligand exchange between the $Ce(acac)_3$ and $Zr(OBu^n)_4$ used as precursors. The presence of acetylacetonato ligands also affects strongly the structural evolution during the pyrolysis and modifies the mechanisms of the release of the residuals deriving from the butoxide of zirconium, which otherwise should form the related alcohol. The butoxides are eliminated as butene above 400 °C, when the steric hindrance of the bulky acac ligands around the metal atoms is reduced. In fact, the acac groups pyrolyze mainly in the range from 300 to 350 °C, even if a low amount remains bonded to the metals until over 500 °C.

Solid-state reactions in the coordination sphere of the transition metal are inferred from the analysis of the decomposition products, particularly in order to explain the formation of aromatic species at higher temperature. The evolution of benzene, toluene, xylene, and trimethylbenzene is common to the pyrolysis of $Zr(acac)_4$, studied merely for elucidating the decomposition mechanisms of acetylacetonato groups.

The morphology, shrinkage, and microstructural and structural features of the gel change through the different thermal treatments, depending on the temperature and atmosphere. The samples thermally treated in a nonoxidizing atmosphere are amorphous and contain some organic moieties, whereas those treated in air are crystalline. The organic functionalities are involved in hydrolysis and condensation reactions, leading to a more interconnected ceramic network. This explains the improvement of the corrosion resistance in acidic environment of steel protected by the amorphous coatings. In this respect, this study contributes to the elucidation of the previous findings regarding the better performance of $ZrO_2$−$CeO_2$ coatings on steel, prepared from gels treated under a vacuum.[4]

**Acknowledgment.** The authors thank Dr. Stefano Gialanella for TEM measurements and the helpful discussion.

CM980187H